ORIGINAL ARTICLE

Mechanical characterization of FDM parts through instrumented flat indentation

Francesco Lambiase[1] · Silvia Ilaria Scipioni[1] · Alfonso Paoletti[1]

Abstract

Evaluating local mechanical properties of parts made by additive manufacturing processes can improve the deposition conditions. This study proposes a non-destructive characterization test to determine the mechanical behavior of fused deposition modeling (FDM) components. Indentation and compression tests were conducted on samples produced by the FDM process, which were created by varying the material flow during the deposition. An empirical relationship was determined between yield strength determined through compression and indentation tests. $R^2 = 0.92$ characterized the correlation between the compression and indentation test. The results indicated that both the yield strength measured through compression tests and that measured by the indentation tests increased linearly with the density of the components. Indentation tests provided more insights concerning the tested surface's local characteristics than the compression test.

1 Introduction

In recent years, significant efforts have been spent to enhance the mechanical behavior of parts made by additive manufacturing (AM) processes. This is due to the new rule exerted by these components and the potential to use these products as finished parts in several fields. After the early application for rapid prototyping purposes, AM components are increasingly employed for rapid tooling and final products. These new applications exploit the potential of AM as compared to conventional processes, including excellent design flexibility, high degree of customization, low or even null fixed costs (depending on the process), no need for specific equipment, excellent availability of machines, distributed production, and lightweight devices [1–3]. On the other hand, the widespread adoption of components produced through AM processes still needs to be improved by issues concerning process standardization, repeatability of the deposition conditions, porosities, and adhesion between the layers. This

often reduced the mechanical behavior of the components, as well as geometrical issues, e g., shrinkage and warpage (especially for processes involving thermal cycles).

Among different AM processes available for producing plastic components, fused deposition modeling (FDM) is increasingly adopted to produce structural components. This is due to the high mechanical performance achievable, since the possibility to manufacture engineering plastics such as PC and PA; techno-polymers such as PEEK [4–9], PEI [10–16], and PAEK [17, 18]; and reinforced plastics [19–25] with discontinuous and continuous fibers. In addition, FDM is easily scalable, and components of excellent dimensions can also be produced through this technology. Finally, FDM can be intrinsically involved in the circular economy loop [26–32] since the raw material can be easily recycled and reused after the end-of-life of the component or "print failures." Compared to other AM processes of polymers (e.g., powder bed fusion, stereolithography, material, jetting), FDM components are affected by specific issues such as poor surface finish and larger porosities. This is due to the larger dimension of the standard nozzles (generally having a diameter between 0.3 and 0.6 mm) used in FDM compared to the dimensions of the laser beams used in SLA and powder bed fusion (typically lower than 0.1 mm). Such porosities severely affect the statical and dynamic

---

✉ Francesco Lambiase
  francesco.lambiase@univaq.it

1 Dept. of Industrial and Information Engineering
   and Economics, University of L'Aquila, via G. Gronchi 18,
   Zona Industriale di Pile, 67100 AQ L'Aquila, Italy

mechanical behavior of the components. In addition, during the deposition process, the pressure exerted by the material on the underlying layer is relatively low (especially if compared to that involved in the injection molding process). This is still more limiting for the adhesion between the layers than other AM processes leading to even more anisotropic behavior [33] of the components. This also involves different fracture mechanisms when the components are loaded along or perpendicular to the growing direction [34].

The presence and dimension of the porosities are not easily predictable in the FDM process since the deposition conditions depend on the selected process parameters as well as the geometry of the component. Figure 1 depicts two parts with different geometries printed under the same process parameters. As can be inferred, the part described in Fig. 1a shows numerous voids, while that reported in Fig. 1b is less affected by the presence of these defects. This indicates the great rule exerted by the component's geometry and the deposition strategy on the voids. Thus, the defects' amount and dimension do not depend on the sole deposition condition. Still, it also greatly depends on the complexity of the component (such as concave-convex features) and the relative dimension of these geometrical features compared to the nozzle diameter.

This also hinders the possibility of determining the mechanical characteristics of a component by testing a "standard" sample that should be representative of the actual component [35]. Besides, since the high plasticity of materials involved in FDM, machining a sample from the actual component is also challenging. The components are duplicated to be produced with material waste. In addition, this approach would be highly time-consuming, requires additional machining equipment (e.g., turning or milling machine), and is less practical. Non-destructive testing (NDT) of the actual component is highly demanded to provide reliable information concerning the component's behavior [36, 37]. Different methods have been adopted to characterize the mechanical behavior of the parts made by
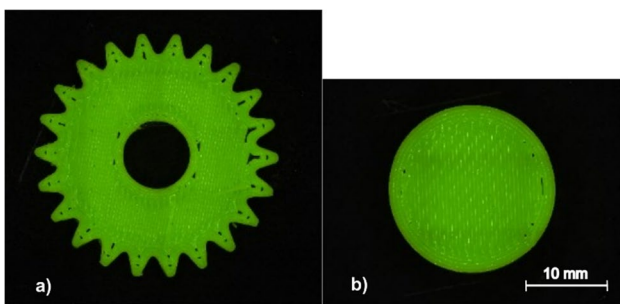
FDM and the relationship with the porosity, including X-ray computed tomography analysis [38] and cross-sectional analysis [35]. Alternatively, non-destructive characterization tests (such as hardness tests) are performed through a technological test that does not directly measure a mechanical characteristic. On the other hand, the measurements from these tests can be correlated to mechanical behavior [39–45]. Compared to conventional tests (e.g., tensile tests, compression tests), non-destructive testing would provide the additional advantage of determining the local property of the actual component [46, 47]. This is particularly important for testing materials with highly inhomogeneous properties, such as those produced through the FDM process. Among them, indentation tests have shown a great capability to predict the mechanical behavior of metals and plastics [48] and even the amount of porosity [35]. Even though instrumented indentation tests were successfully involved to determine the yield strength of full density materials, the applicability of this approach to porous media has been not proved yet.

The present investigation aims to evaluate the suitability of instrumented indentation tests to determine the local compressive behavior of components made by the FDM process. To this end, a campaign of experimental tests was conducted by varying the density of the samples and determining the mechanical behavior of the components through standard compressive tests and instrumented flat indentation. Morphological analysis of the samples was also conducted through optical microscopy to investigate the influence of the surface morphology on the determined mechanical properties. Finally, an empirical model was established to predict compressive behavior through indentation tests.

2 Materials and methods

The study was conducted on cylindrically shaped specimens made of PLA produced by Fabbrix. Cylindrical specimens were produced for compression and flat indentation tests. The samples were 20 mm in diameter and 40 mm in height according to ASTM 695 standards. These dimensions were selected to have the edge of the indenter to the sample border at least two times the diameter of the indenter (to limit the sample size effect), as shown in Fig. 2.

Samples were produced using two commercial machines Creality Ender 6, setting the extruder temperature at 210 °C and bed temperature at 60 °C. The speed was set to 4000 mm/min, while the layer width was set to 0.2 mm, half the nozzle's diameter (0.4 mm). The specimens were made with 100% rectilinear fill, generating three perimetral shells with a fixed width of 0.5 mm. Figure 3 depicts the deposition strategy adopted for the sample printing.

Commercial software Simplify 3D was used to set the printing parameters and generate the GCODE used as input

Fig. 1 Influence of the component geometry on the presence of defects — macrographs of two components made with the same deposition strategy and different shapes: **a** concave profile; **b** convex profile

for the FDM machines. A campaign of experimental tests was performed by varying the extrusion multiplier. This parameter allows for controlling the material flow deposited during printing. Specimens with extrusion multipliers between 99 and 104% were analyzed. Four specimens were printed for each extrusion multiplier value. After printing, all specimens were weighed using a precision balance model XT1220M by Precisa, and the dimensions of the specimens were measured through a micrometer. This enabled calculating the sample's density and the influence of the extrusion multiplier on the density.

Compression tests were performed according to ASTM D695 standards with a traverse speed of 1 mm/s using MTS's Universal Testing Machine model C43.50. Instrumented flat indentation tests were performed at a constant travel speed of 0.1 mm/min, using a flat-end cylindrical indenter with 4.0 mm diameter made of K720 high-strength steel by Bohler. The diameter of the indenter was selected based on the previous study [35]. The adoption of smaller indenters (i.e., 2 mm in diameter) led to lower test reliability since the results were susceptible to the surface morphology of the samples. A pre-load of 200 N was used to avoid contact-dependent trends such as the non-coplanarity between the sample surface and the indenter flat face.

Instrumented indentation tests were performed on the flat specimen's surfaces, as shown in Fig. 2. Indentation tests were performed on the upper and bottom surfaces of the specimen, imposing a maximum penetration depth of 2.0 mm. Load–displacement curves were recorded during the tests, as shown in Fig. 4. An algorithm was developed to perform feature extraction from the curves using MATLAB 2022b environment.

The yield strength from compressive tests was determined according to the ASTM D695 standards, as schematically shown in Fig. 4.

Despite compression tests, whereas the stress is monodirectional, an uneven stress distribution is produced on the sample during the indentation test. Consequently, the stress of the material underlying the indenter is due to both elastic and plastic deformation. In the beginning, elastic deformation is predominant, then as sufficient indentation depth is reached, plastic deformation localizes around the indenter edge [49] and then enlarges for further indentation depth.

To determine the material's properties, the load was divided by the surface area of the flat indenter, as shown in Fig. 5. The load shows a smoother transition between the linear elastic behavior and the onset of yielding. The first part of the loading load–displacement curve is almost linear due to the high elastic contribution. As the test proceeds (increasing the penetration depth), the curve approaches a plateau corresponding to a significant material flow. Thus, two approaches were followed to determine the onset of the yielding condition: the deviation from the linear regime
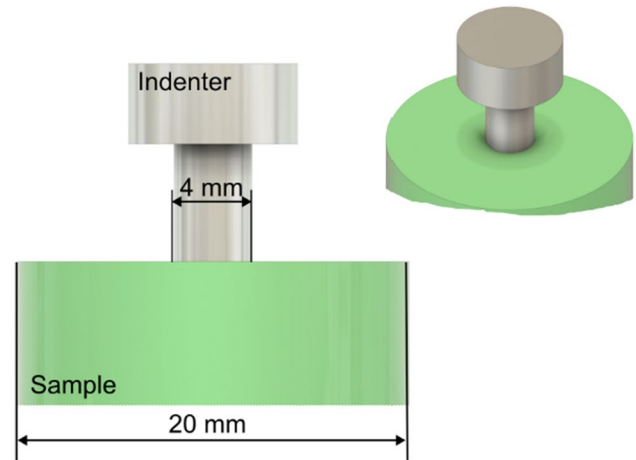

Fig. 2 Schematic of the tool and the sample during the flat indentation test
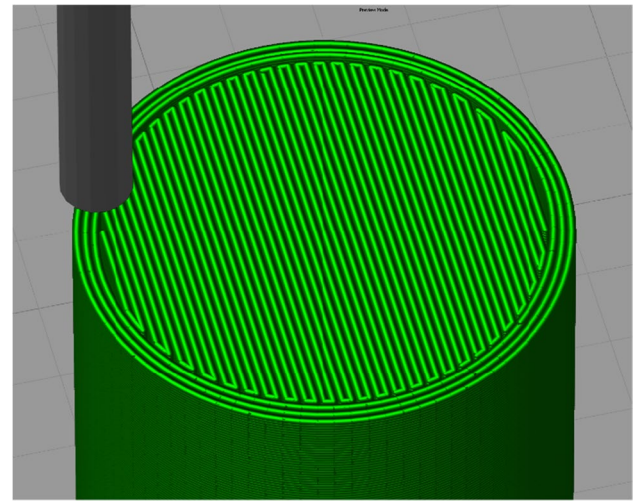

Fig. 3 Schematic of the adopted sample deposition strategy showing three perimeter shells and a 100% rectilinear infill
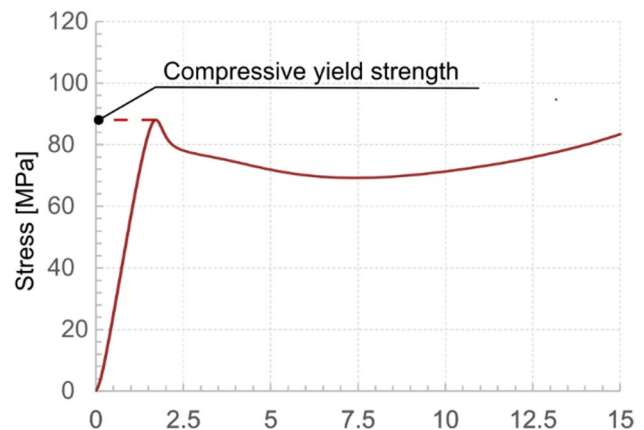

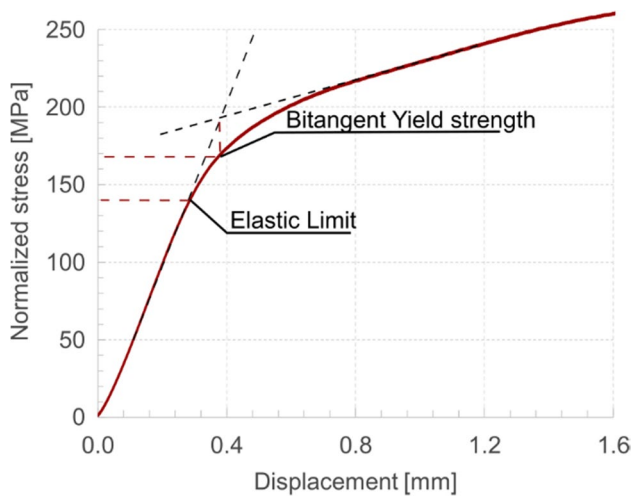**Fig. 4** Stress-displacement curve recorded during compression tests

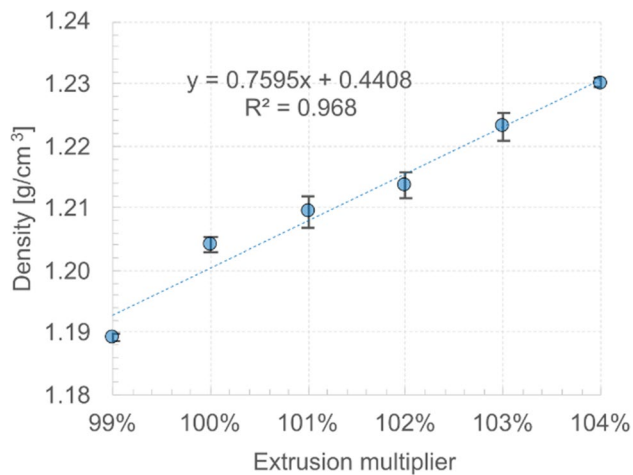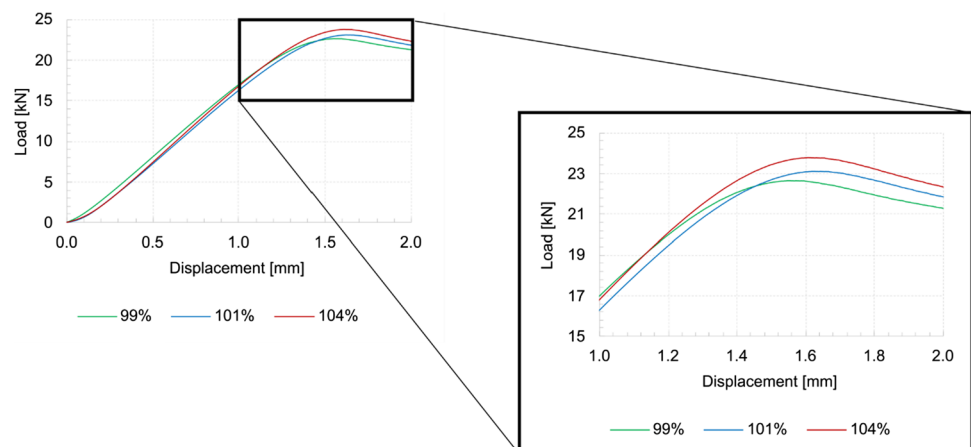**Fig. 5** Normalized stress curve recorded during flat indentation tests

Fig. 6 Variation of the density as a function of the extrusion multipliers using different printers. (Density of the filament as reported by the supplier is 1.25 g/cm.[3])

(elastic limit) and the bitangent yield strength, as shown in Fig. 5. These values were determined automatically through a routine developed in MATLAB 2022b.

3 Results

The influence of the extrusion multiplier on the density of the samples is shown in Fig. 6. The density shows linear growth with the extrusion multiplier, with values starting from 1.19 up to 1.23 g/cm^3.

3.1 Mechanical tests

Figure 7 compares the load–displacement curves recorded during the compression tests for samples achieved with different extrusion multipliers (i.e., 99%, 101%, and 104%). The higher the extrusion multiplier, the higher the stiffness and the peak load. This was due to the higher density of the samples produced with higher extrusion multipliers.

The influence of the extrusion multiplier and density on the yield strength measured through the compression test are depicted in Fig. 8 a and b. The yield strength showed a linear increase versus both the extrusion multiplier and the density of the specimens. The specimens printed with a 99% extrusion multiplier showed yield strength of 71 MPa; increasing the value of the extrusion multiplier by 5% led to an increase of yield strength up to 75 MPa, corresponding to an increase of yield strength up to 5%.

Figure 9 compares the load–displacement curves recorded during the indentation tests for samples achieved with different extrusion multipliers (i.e., 99%, 101%, and 104%). As for the compression tests, the higher the extrusion multiplier (and the density of the sample), the higher the load exerted on the sample during the indentation. From the observation of the curves, it emerges that the intersection of the tangents to the curves is reached

Fig. 7 Force–displacement curves recorded during the compression tests of samples printed with different extrusion multipliers

Fig. 8 Influence of the **a** extrusion multiplier and **b** density on the yield strength measured through compression tests
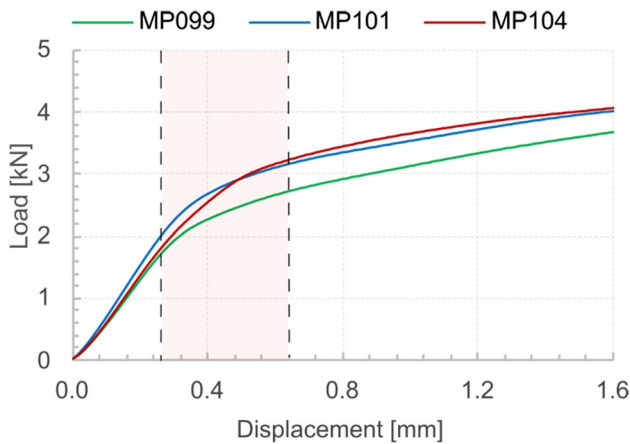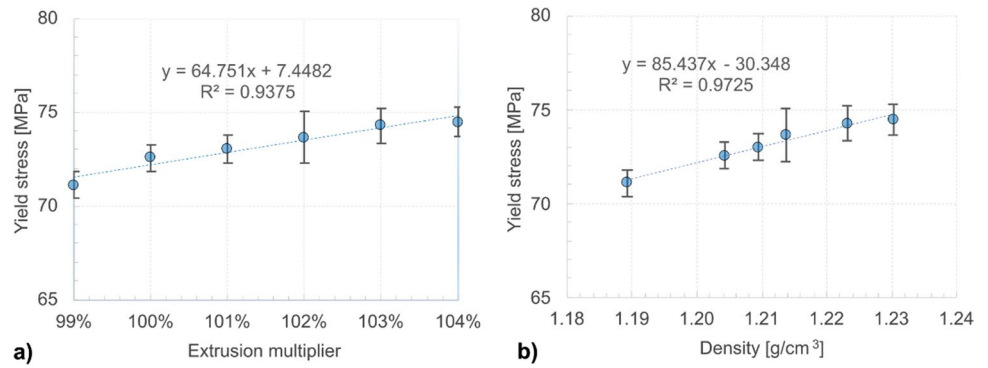

Fig. 9 Load–displacement curves recorded during the indentation tests of samples printed with different extrusion multipliers

in correspondence of displacement between 0.2 mm and 0.6 mm, as shown by the red rectangle in Fig. 9. Thus, a maximum indentation depth of 0.8 mm could be enough to determine the yielding condition through indentation tests using the bitangent method, while 0.4 mm would be required if the elastic limit is preferred.

As described in Sect. 2, each test's yielding condition was determined through a Matlab routine. Figure 10 a and b depict the influence of the extrusion multiplier on the normalized stress measured through indentation tests performed on the upper and lower sample surface using the two methods to detect the yielding onset.

The normalized strength, which was determined through the bitangent method, measured on the upper surface of the samples (Fig. 10a) increased almost linearly with the extrusion multiplier. The average yield strength for EM = 99%

Fig. 10 Influence of the extrusion multiplier on the normalized force determined through indentation tests performed on the **a–c** top surface and **b–d** bottom surface
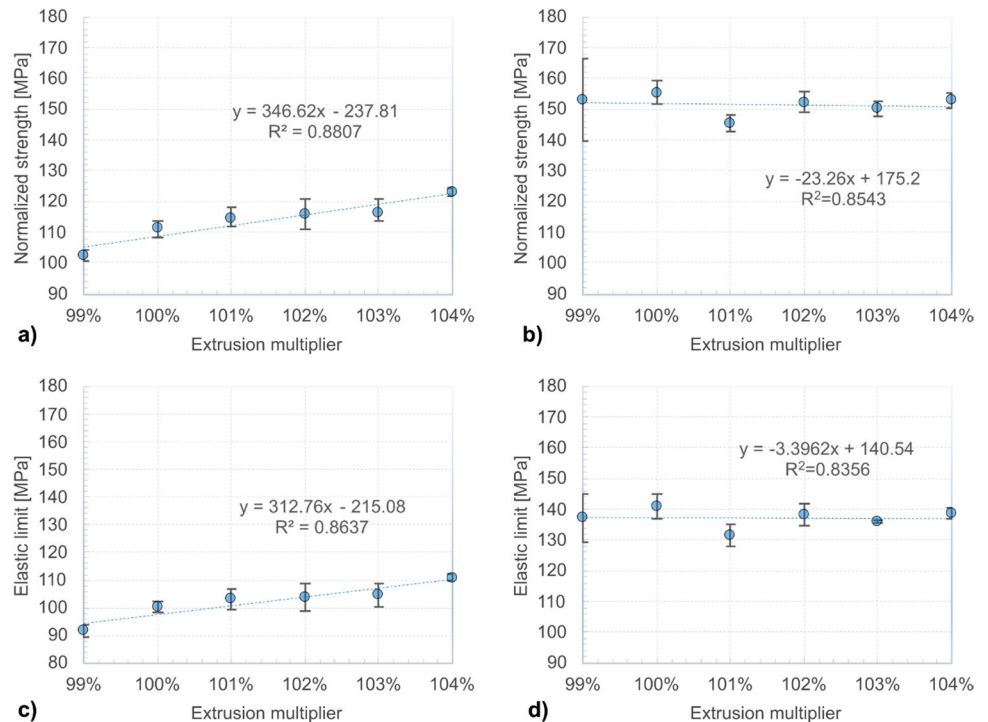
was 102 N/mm², while the average yield strength for EM = 104% was 123 N/mm², corresponding to an increase of 21%. On the other hand, the normalized stress measured on the bottom surface of the specimens showed lower sensitivity to the extrusion multiplier during the indentation test. Indeed, the yield strength values hold almost constant. The average yield strength, calculated through the bitangent method, determined on the lower face of the specimens was equal to 152 MPa, and the standard deviation was 3 MPa. This indicated that the mechanical properties of the component surface in contact with the building plate are almost unaffected by the adopted extrusion multiplier and are much higher than those measured on the upper surface. Similar trends (with lower values) were found by adopting the elastic limit method. Indeed, the elastic limit increased significantly on the upper surface with the EM, while it showed lower sensitivity in the indentation tests performed on the bottom surface.

3.2 Morphological analysis of the sample's surfaces

Figure 11 depicts the upper and bottom surfaces of samples produced with $EM = 99\%$ and $EM = 104\%$. The upper surface of the sample made using $EM = 99\%$ (depicted in Fig. 11a) shows some unfilled regions in correspondence of the external shells and the internal infill. Adopting the same strategy with a higher extrusion multiplier, $EM = 104\%$ (as shown in Fig. 11b) indicates that the surface is more regular without unfilled regions. Figure 11 c and d depict the bottom surface of the samples with $EM = 99\%$ and $EM = 104\%$, respectively. These surfaces were very similar, and no unfilled regions were detected regardless of the adopted extrusion multiplier.

To further investigate the differences among the surfaces of the samples produced with different extrusion multipliers and through other EM, morphological analysis was performed through 3D surface reconstruction.

Fig. 11 Macrograph of surfaces of samples made with $EM = 99\%$: **a** upper; **b** bottom and $EM = 104\%$: **c** upper and **d** bottom
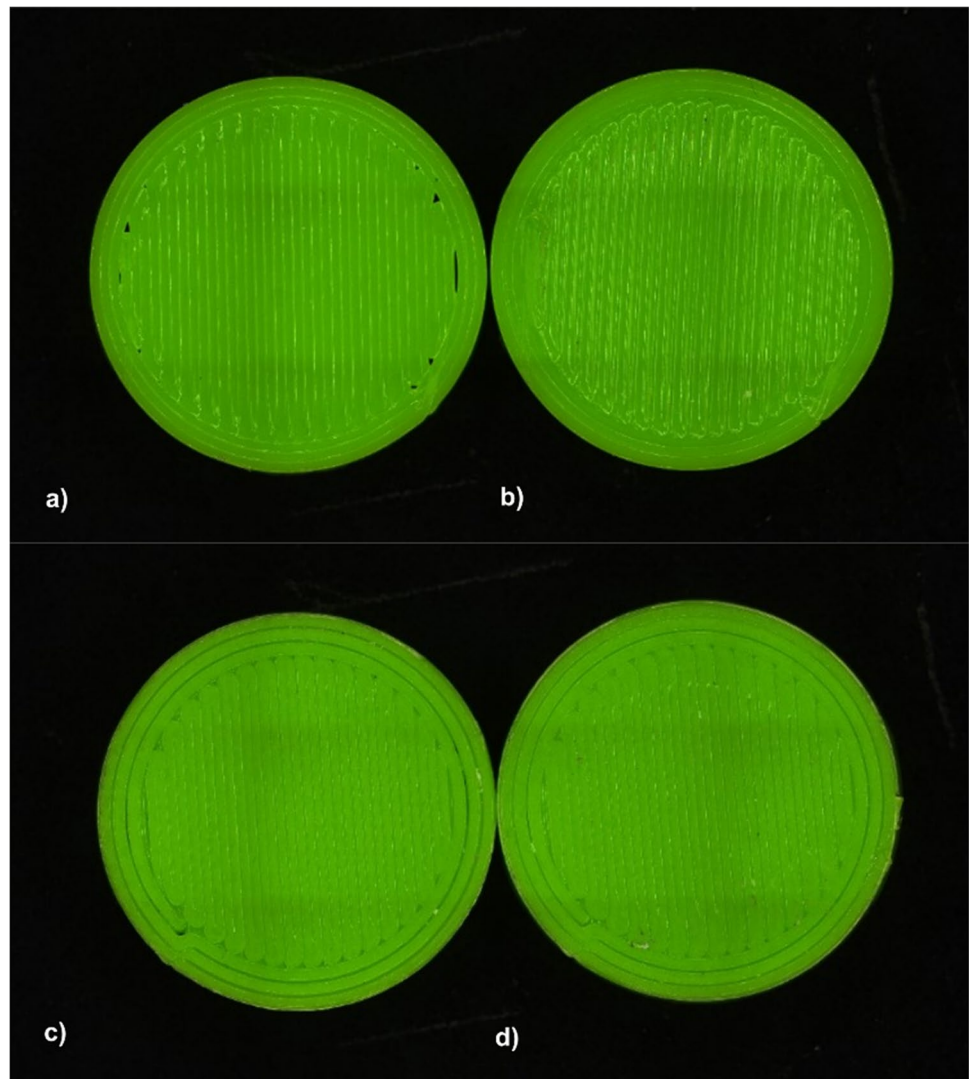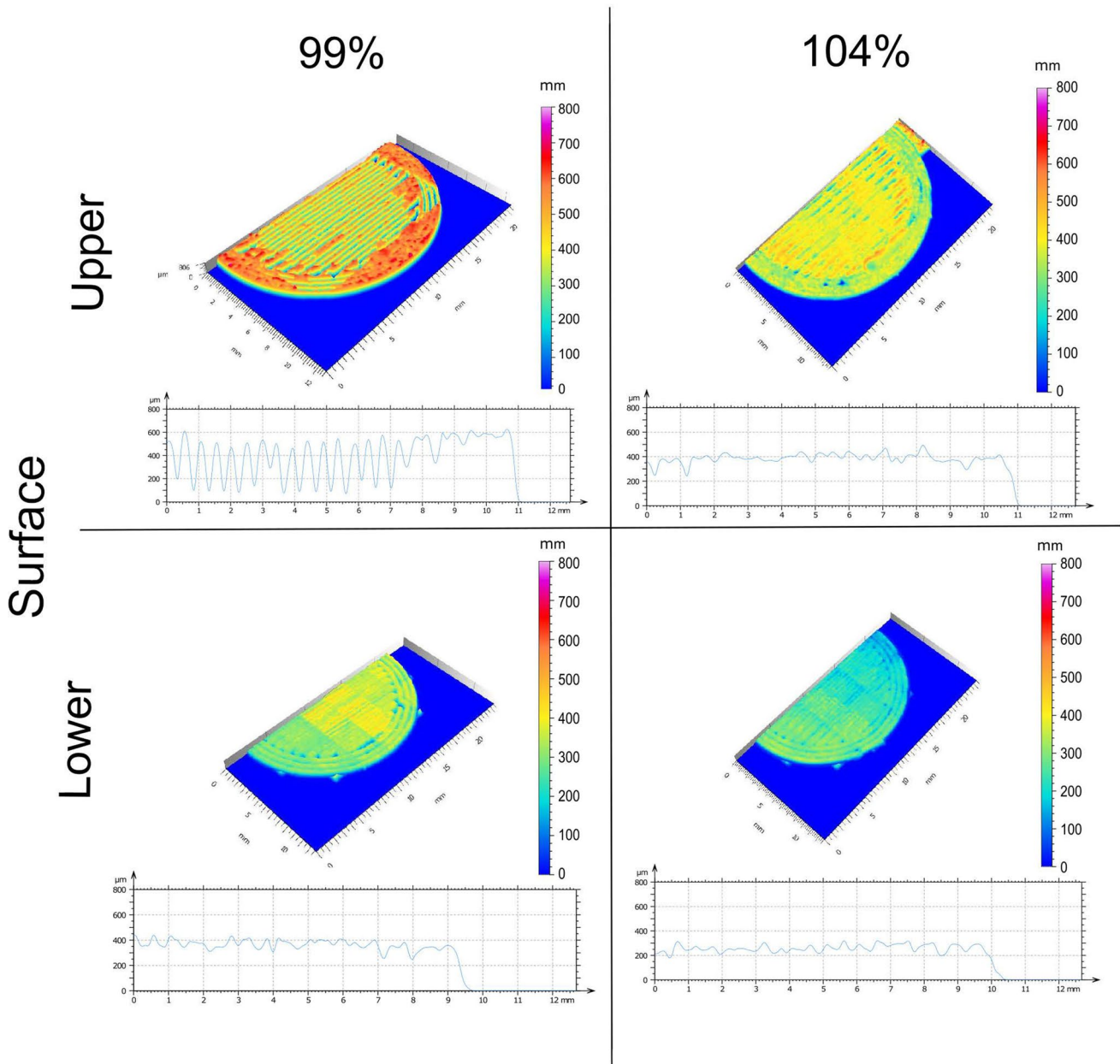
Fig. 12 3D maps of the upper and lower surfaces on samples produced with EM = 99% and EM = 104%

Figure 12 depicts the 3D maps of the reconstructed surfaces on two samples (*EM* = 99% and *EM* = 104%) on the upper and bottom surfaces (please note that all the maps have the same limits).

The upper surface of the sample made with *EM* = 99% shows the presence of peaks and valleys indicative of the deposited direction. Indeed, the virtual cross-section shows a sinusoidal-like profile with an average amplitude of almost 400 mm. On the other hand, the upper surface of the sample made with *EM* = 104% shows a more uniform morphology, as indicated by the virtual cross-section. These measurements indicate that the adopted extrusion multiplier strongly influences the morphology of the upper surface during the deposition and, consequently, the stiffness of the deposited layer. Otherwise, comparing the 3D maps of the bottom surface, it emerges that the adopted extrusion multiplier less influences the morphology of these surfaces.

The above results indicate that the upper and bottom surfaces show different mechanical behavior owing to the

different deposition conditions. Indeed, the bottom surface is produced by extruding material against the building plate; on the other hand, the upper surface is printed over previously deposited layers (which are much softer and can still be under a rubber-like state). During FFF process, the building plate temperature was set at 60 °C. This temperature was above the glass transition temperature of the PLA (55 °C). This enabled the polymer's molecular chains close to the plate to rearrange during the entire printing process, providing a more "compact" chain distribution. On the other hand, the overlying layers' material rapidly cools down after being deposited. These layers do not have sufficient time to let the polymer chains rearrange in a more compact form. This leads to uneven mechanical properties between the material in contact with the building plate and the overlying materials.

The compression test averages such local differences, while the indentation test can discern such local behavior more easily.

3.3 Correlation between the compression and indentation tests

Figure 13a and b depict the normalized strength and the elastic limit as a function of sample density, respectively. The normalized strength grows linearly as a function of density. Similar trends can also be observed between the elastic limit and the density of the samples. In both cases, the coefficient of determination was relatively high. For both the normalized strength (calculated through the

bitangent method) and the elastic limit, $R^2 \cong 0.94$. On the other hand, both the normalized strength and the elastic limit measured on the bottom sample surface are almost unaffected by the average density of the sample.

Thus, for each sample, the yield strength measured through compression tests was compared to the yield strength measured by indentation tests performed on the upper surface under the same deposition conditions.

Figure 14 shows the correlation between the yield strength obtained through the indentation test and that obtained during the compression test. The correlation between the two yield strengths showed a linear trend, with a coefficient R^2 of 0.92. Similarly, the elastic limit (measured by the indentation test) and the yield strength (measured through the compression test) also showed a significant correlation since the coefficient of determination R^2 was 0.90.

Thus, the established relationship (linear regression coefficients) can be exploited to convert the yielding condition measured through indentation tests to predict the compressive yield strength of the actual component on a specific location.

4 Discussion

Among different AM processes, fused deposition modeling is gaining great diffusion since different advantages over other AM processes of plastics, including the more effortless scalability, higher material deposition rate, possibility to produce reinforced plastics even with long fibers, chance to

Fig. 13 Influence of the sample density on the yielding condition measured by indentation tests performed on the **a**, **b** upper and **c**, **d** lower sample surface
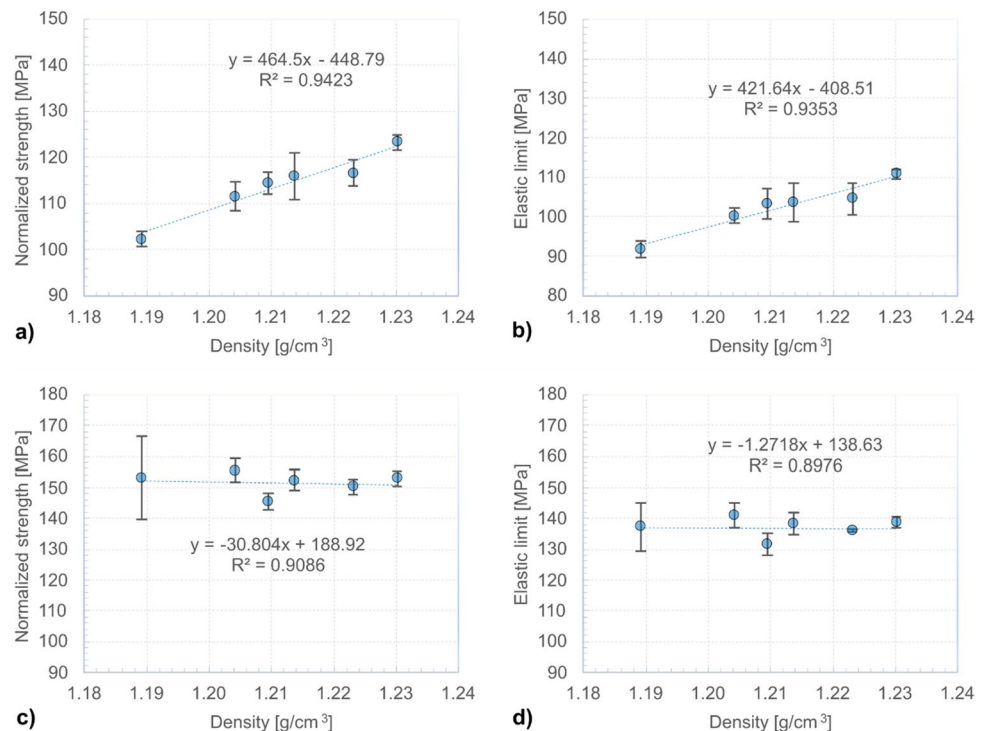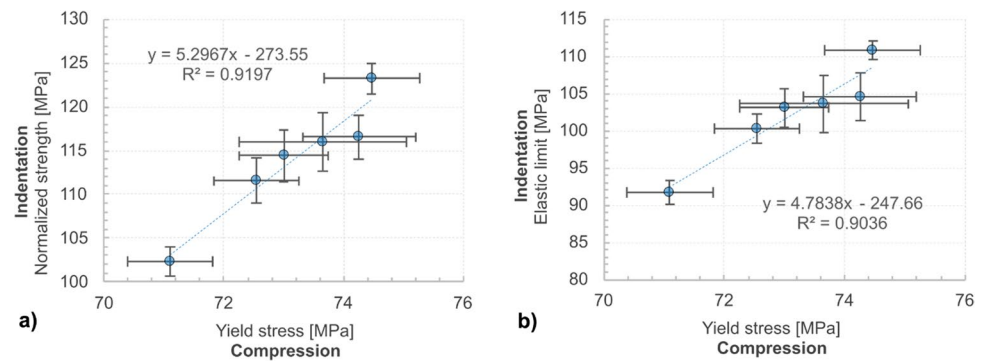
Fig. 14 Correlation between the **a** yield strength (measured through the compression tests) and **b** the normalized force (measured through the indentation tests)

embed electrical circuits or other materials, and the broader availability of raw materials and lower costs.

The growing adoption of additive manufacturing components for structural applications is rapidly pushing attention to product qualification and the assessment of mechanical behavior. The mechanical behavior depends on different aspects, including the raw material, process parameters, the adopted AM machine, and the geometry of the component. Thus, adopting reference samples, which are often characterized by simpler geometries, may lead to an unreliable prediction of the mechanical behavior of the actual part. In addition, manufacturing reference samples to perform characterization tests or machining sample tests from the actual component (used as a trial to be eventually reproduced) is highly time-consuming and leads to excellent material waste (other than requiring additional machines such as turning or milling machines). Even though an alternative solution is represented by the development of numerical models based on the X-ray computed tomography analysis to produce a digital twin of the component, this approach is expensive and highly time-consuming.

On the other hand, the development of non-destructive testing can potentially overcome these limitations; it can also provide valuable information concerning the local properties of a component instead of global characteristics. The results from this research indicate that indentation tests can determine a component's local yield strength, and this value can be correlated to the compressive yield strength. Indeed, polymers show great sensitivity to the hydrostatic stress. Thus, since indentation produces a compression rather than tension, it can be better correlated to the compressive properties of the component. Thus, the developed approach is particularly suitable for testing tools made by FFF process since they often bear compressive stress. In addition, once established the relationship between the tensile properties and the density of the components, the indentation tests can also provide local information concerning the tensile strength of the component.

It is important to note that through the indentation test, it is possible to determine the value of the yield strength by fixing the crosshead displacement to a value smaller than 1 mm. This allows for a negligible imprint on the specimen, as shown in Fig. 15, which can be acceptable for the final product.

Furthermore, the coefficient of correlation using the elastic limit method was slightly lower ($R^2 = 0.90$) than that of the bitangent method ($R^2 = 0.92$). Thus, the imprint could be even shallower since the maximum penetration depth could be as low as 0.4 mm; thus, considering the high elasticity of the polymers and the porosity of FDM parts, the plastic imprint can be almost imperceptible as shown in Fig. 15.

5 Conclusions

The present work investigated the suitability of indentation tests to determine the local mechanical behavior of fused deposition modeling (FDM) components. A campaign of indentation and compression tests was conducted on samples produced by the
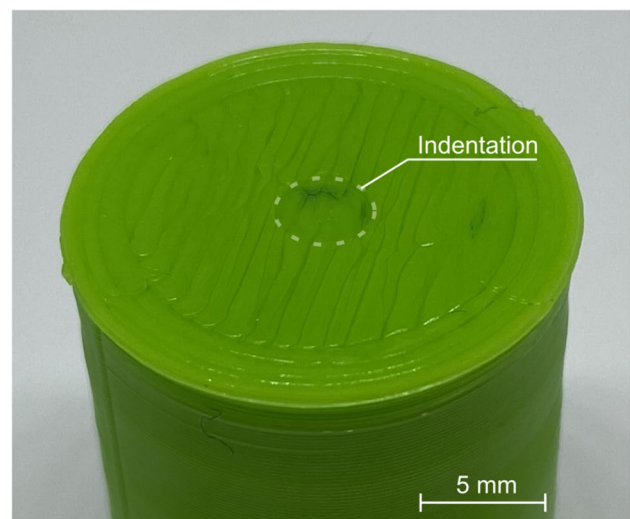

Fig. 15 Picture of the indented surface with an indentation depth of 1.0 mm

FDM process using polylactide acid (PLA), varying the material flow during the deposition. The force–displacement curves were processed through an algorithm that extracted the yield strength values during the compression and indentation tests. The influence of the material flow on the mechanical behavior of specimens was also analyzed. The main results are as follows:

- The extrusion multiplier greatly influenced the yield strength of the FDM specimens. The variation of the extrusion multiplier from 99 to 104% led to an increase in the compressive yield strength from 71 to 75 MPa, corresponding to a percentage increase of 5%.
- The morphology of the upper surfaces of the samples was greatly influenced by the adopted extrusion multiplier. The surface showed a sinusoidal shape due to the unfilled regions for lower values of the extrusion multiplier. As the extrusion multiplier increased, the surface was more uniform. On the other hand, the morphology of the bottom surface was almost unaffected by the extrusion multiplier. This difference was due to different deposition conditions occurring at the beginning of the process (the material is extruded over the building plate) and subsequent layers' deposition.
- The yield strength value obtained during the indentation test on the upper surface of specimens grew linearly with the density of the specimens; the normalized strength value ranged from 102 to 124 MPa, for specimens printed with the extrusion multipliers of 99% and 104%, respectively. On the other hand, the yield strength measured through the indentation tests on the bottom surface was negligibly influenced by the extrusion multiplier.
- An empirical relationship between the yield strength measured through the compression test and the normalized strength determined during the indentation test was determined. The coefficient of determination $R^2 = 0.92$; this indicates that the indentation tests can be successfully employed to determine the local properties of the components made by FDM. In addition, since indentation tests can release relatively shallow indentation (as small as 0.4 mm in depth), the described procedure can be used as a non-destructive mechanical test for FDM components.

Declarations

Ethical approval Not applicable.

Consent to participate Not applicable.

Consent for publication Not applicable.

Competing interests The authors declare no competing interests.

References

1. Perez-Mananes R, Jose SGS, Desco-Menendez M, Sanchez-Arcilla I, Gonzalez-Fernandez E, Vaquero-Martin J, Gonzalez-Garzon JP, Mediavilla-Santos L, Trapero-Moreno D, Calvo-Haro JA (2021) Application of 3D printing and distributed manufacturing during the first-wave of COVID-19 pandemic. Our experience at a third-level university hospital. 3D Print Med 7(1):7

2. Durão LFCS, Christ A, Anderl R, Schützer K, Zancul E (2016) Distributed manufacturing of spare parts based on additive manufacturing: use cases and technical aspects. Procedia CIRP 57:704–709

3. Wittbrodt BT, Glover AG, Laureto J, Anzalone GC, Oppliger D, Irwin JL, Pearce JM (2013) Life-cycle economic analysis of distributed manufacturing with open-source 3-D printers. Mechatron 23(6):713–726

4. Berretta S, Davies R, Shyng YT, Wang Y, Ghita O (2017) Fused deposition modelling of high temperature polymers: exploring CNT PEEK composites. Polym Test 63:251–262

5. Rinaldi M, Ghidini T, Cecchini F, Brandao A, Nanni F (2018) Additive layer manufacturing of poly (ether ether ketone) via FDM. Compos Part B: Eng 145:162–172

6. Geng P, Zhao J, Wu W, Ye W, Wang Y, Wang S, Zhang S (2019) Effects of extrusion speed and printing speed on the 3D printing stability of extruded PEEK filament. J Manuf Process 37:266–273

7. Zanjanijam AR, Major I, Lyons JG, Lafont U, Devine DM (2020) Fused filament fabrication of PEEK: a review of process-structure-property relationships. Polymers (Basel) 12(8):1665

8. Zhao Y, Zhao K, Li Y, Chen F (2020) Mechanical characterization of biocompatible PEEK by FDM. J Manuf Process 56:28–42

9. Dua R, Rashad Z, Spears J, Dunn G, Maxwell M (2021) Applications of 3D-printed PEEK via fused filament fabrication: a systematic review. Polym (Basel) 13(22):4046

10. Fischer M, Schöppner V (2016) Fatigue behavior of FDM parts manufactured with Ultem 9085. Jom 69(3):563–568

11. Zaldivar RJ, Witkin DB, McLouth T, Patel DN, Schmitt K, Nokes JP (2017) Influence of processing and orientation print effects on the mechanical and thermal behavior of 3D-Printed ULTEM® 9085 Material. Addit Manuf 13:71–80

12. Cicala G, Ognibene G, Portuesi S, Blanco I, Rapisarda M, Pergolizzi E, Recca G (2018) Comparison of Ultem 9085 used in

fused deposition modelling (FDM) with polytherimide blends. Materials (Basel) 11(2):285

13. Gebisa AW, Lemu HG (2018) Investigating effects of fused-deposition modeling (FDM) processing parameters on flexural properties of ULTEM 9085 using designed experiment. Mater (Basel) 11(4):500

14. Wu H, Sulkis M, Driver J, Saade-Castillo A, Thompson A, Koo JH (2018) Multi-functional ULTEM™1010 composite filaments for additive manufacturing using Fused Filament Fabrication (FFF). Addit Manuf 24:298–306

15. Chueca de Bruijn A, Gómez-Gras G, Pérez MA (2020) Mechanical study on the impact of an effective solvent support-removal methodology for FDM Ultem 9085 parts. Polym Test 85:106433

16. McLouth TD, Gustafson SM, Kim HI, Zaldivar RJ (2021) Enhancement of FDM ULTEM® 9085 bond strength via atmospheric plasma treatment. J Manuf Process 66:179–188

17. Prechtel A, Reymus M, Edelhoff D, Hickel R, Stawarczyk B (2020) Comparison of various 3D printed and milled PAEK materials: effect of printing direction and artificial aging on Martens parameters. Dent Mater 36(2):197–209

18. Garcia-Leiner M, Streifel B, Başgül C, MacDonald DW, Kurtz SM (2021) Characterization of polyaryletherketone (PAEK) filaments and printed parts produced by extrusion-based additive manufacturing. Polym Int 70(8):1128–1136

19. Luke SS, Soares D, Marshall JV, Sheddden J, Keleş Ö (2021) Effect of fiber content and fiber orientation on mechanical behavior of fused filament fabricated continuous-glass-fiber-reinforced nylon. Rapid Prototyp J 27(7):1346–1354

20. Brounstein Z, Yeager CM, Labouriau A (2021) Development of antimicrobial PLA composites for fused filament fabrication. Polym (Basel) 13(4):580

21. Angelopoulos PM, Samouhos M, Taxiarchou M (2021) Functional fillers in composite filaments for fused filament fabrication; a review. Mater Today: Proc 37:4031–4043

22. Zhang X, Fan W, Liu T (2020) Fused deposition modeling 3D printing of polyamide-based composites and its applications. Compos Commun 21:100413

23. Penumakala PK, Santo J, Thomas A (2020) A critical review on the fused deposition modeling of thermoplastic polymer composites. Compos Part B: Eng 201:108336

24. Hu C, Qin Q-H (2020) Advances in fused deposition modeling of discontinuous fiber/polymer composites. Curr Opin Solid State Mater Sci 24(5):100867

25. Dickson AN, Abourayana HM, Dowling DP (2020) 3D printing of fibre-reinforced thermoplastic composites using fused filament fabrication-a review. Polym (Basel) 12(10):2188

26. Zhu C, Li T, Mohideen MM, Hu P, Gupta R, Ramakrishna S, Liu Y (2021) Realization of circular economY of 3D printed plastics: a review. Polym (Basel) 13(5):744

27. Yadav D, Garg RK, Ahlawat A, Chhabra D (2020) 3D printable biomaterials for orthopedic implants: solution for sustainable and circular economy. Resour Policy 68:101767

28. Shanmugam V, Das O, Neisiany RE, Babu K, Singh S, Hedenqvist MS, Berto F, Ramakrishna S (2020) Polymer recycling in additive manufacturing: an opportunity for the circular economy. Mater Circ Econ 2:11

29. DePalma K, Walluk MR, Murtaugh A, Hilton J, McConky S, Hilton B (2020) Assessment of 3D printing using fused deposition modeling and selective laser sintering for a circular economy. J Clean Prod 264:121567

30. Cruz Sanchez FA, Boudaoud H, Camargo M, Pearce JM (2020) Plastic recycling in additive manufacturing: a systematic literature review and opportunities for the circular economy. J Clean Prod 264:121602

31. Colorado HA, Velásquez EIG, Monteiro SN (2020) Sustainability of additive manufacturing: the circular economy of materials and environmental perspectives. J Market Res 9(4):8221–8234

32. Fonseca DA, Simões FJP (2019) Direct digital manufacturing in the context of a circular economY. Appl Mech Mater 890:21–33

33. Domingo-Espin M, Puigoriol-Forcada JM, Garcia-Granada A-A, Llumà J, Borros S, Reyes G (2015) Mechanical property characterization and simulation of fused deposition modeling Polycarbonate parts. Mater Des 83:670–677

34. Al-Maharma AY, Patil SP, Markert B (2020) Effects of porosity on the mechanical properties of additively manufactured components: a critical review. Mater Res Express 7(12):122001

35. Lambiase F, Scipioni SI, Paoletti A (2022) Determination of local density in components made by fused deposition modeling through indentation test. Int J Adv Manuf Technol 122(3–4):1467–1478

36. Duarte VR, Rodrigues TA, Machado MA, Pragana JPM, Pombinha P, Coutinho L, Silva CMA, Miranda RM, Goodwin C, Huber DE, Oliveira JP, Santos TG (2021) Benchmarking of nondestructive testing for additive manufacturing. 3D Print Addit Manuf 8(4):263–270

37. Sorger GL, Oliveira JP, Inácio PL, Enzinger N, Vilaça P, Miranda RM, Santos TG (2019) Non-destructive microstructural analysis by electrical conductivity: comparison with hardness measurements in different materials. J Mater Sci Technol 35(3):360–368

38. Wang X, Zhao L, Fuh JYH, Lee HP (2019) Effect of porosity on mechanical properties of 3D printed polymers: experiments and micromechanical modeling based on X-ray computed tomography analysis. Polym (Basel) 11(7):1154

39. Scales M, Anderson J, Kornuta JA, Switzner N, Gonzalez R, Veloo P (2022) Accurate estimation of yield strength and ultimate tensile strength through instrumented indentation testing and chemical composition testing. Mater (Basel) 15(3):832

40. Germann J, Bensing T, Moneke M (2022) Correlation between scratch behavior and tensile properties in injection molded and extruded polymers. Polym (Basel) 14(5):1016

41. Liu X, Cai L, Chen H, Si S (2020) Semi-analytical model for flat indentation of metal materials and its applications. Chin J Aeronaut 33(12):3266–3277

42. Fu H, Cai L, Chai Z, Liu X, Zhang L, Geng S, Zhang K, Liao H, Wu X, Wang X, Liu D, Chen J (2020) Evaluation of bonding properties by flat indentation method for an EBW joint of RAFM steel for fusion application. Nucl Mater Energy 25:100861

43. Clausner A, Richter F (2015) Determination of yield stress from nano-indentation experiments. Eur J Mech A Solids 51:11–20

44. Rodríguez M, Molina-Aldareguía JM, González C, Llorca J (2012) Determination of the mechanical properties of amorphous materials through instrumented nanoindentation. Acta Mater 60(9):3953–3964

45. Lucignano C, Quadrini F (2009) Indentation of functionally graded polyester composites. Meas 42(6):894–902

46. Jin Y, Walker E, Heo H, Krokhin A, Choi T-Y, Neogi A (2020) Nondestructive ultrasonic evaluation of fused deposition modeling based additively manufactured 3D-printed structures. Smart Mater Struct 29(4):045020

47. Butt J, Bhaskar R, Mohaghegh V (2022) Non-destructive and destructive testing to analyse the effects of processing parameters on the tensile and flexural properties of FFF-printed graphene-enhanced PLA. J Compos Sci 6(5):148

48. Alisafaei F, Han C-S (2015) Indentation depth dependent mechanical behavior in polymers. Adv Condens Matter Phys 2015:1–20

49. Riccardi B, Montanari R (2004) Indentation of metals by a flat-ended cylindrical punch. Mater Sci Eng: A 381(1–2):281–291